

## Decay of Grid Turbulence in a Finite Channel

Steven R. Stalp, L. Skrbek, and Russell J. Donnelly

*Cryogenic Helium Turbulence Laboratory, Department of Physics, University of Oregon, Eugene, Oregon 97403*  
(Received 3 September 1998)

We develop a classical model for the decay of homogeneous and isotropic turbulence that takes into account the growth of the energy containing length scale and its saturation when it reaches the size of the containing vessel. The model describes our data on the decay of grid turbulence in helium II through 4 orders of magnitude in vorticity, as well as classical experiments on decaying turbulence. [S0031-9007(99)09342-4]

PACS numbers: 47.27.Gs, 47.37.+q, 67.40.Vs

The decay of homogeneous and isotropic turbulence (HIT) is regarded as one of the fundamental problems of fluid dynamics [1]. Experiments on HIT usually study grid-generated turbulence in wind tunnels as it decays downstream [1]. Other investigations involve measurements of decaying turbulence created by an oscillating grid in water [2]. We propose a model for decaying HIT and present experimental data on the decay of turbulence behind a towed grid in helium II that spans an unprecedented dynamical range.

The kinematic viscosity of helium II,  $\nu$ , based on the total density,  $\rho$ , is nearly 3 orders of magnitude lower than that of air. The low viscosity allows investigation of high Reynolds number turbulence in a relatively small apparatus. A novel technique where turbulence is created by towing a grid through a stationary sample of helium II was first reported in [3]. The authors analyzed the decaying superfluid vorticity from 1 to 5 s and assumed an energy containing length scale constant in time. We have improved this experimental technique in several ways to allow measurements from  $\sim 10^4$  to  $\sim 1$  Hz in vorticity obtained over 3 orders of magnitude in time.

We define the superfluid vorticity as  $\omega(t) = \kappa L$ , where  $\kappa$  is the quantum of circulation and  $L$  is the length of quantized vortex line per unit volume. We obtain  $L$  from the attenuation of second sound using a newly developed model suitable for arbitrary levels of attenuation [4]. Mesh Reynolds numbers as high as  $10^5$  are achieved by towing a grid (mesh size  $M = 0.167$  cm), with grid towing velocity,  $V_g$ , between 5 and 200 cm/s, in a  $1 \times 1 \times 56$  cm<sup>3</sup> channel. Observing the turbulent decay through 3 orders of magnitude in time would be equivalent to observations over  $10^4$  mesh lengths downstream in a classical wind tunnel, making our system unique in the study of turbulence.

In the frame of the phenomenological two-fluid model, helium II consists of two independent fluids: the inviscid superfluid of density  $\rho_s$ , and the normal fluid of dynamic viscosity  $\mu$  and density  $\rho_n$ , where  $\rho = \rho_s + \rho_n$ . However, the presence of quantized vortices couple the two fluids together, via mutual friction, as demonstrated in the well-known rotating bucket experiment. Rotating He II

is threaded by a rectilinear array of quantized vortices so that the superfluid, on average, is also in solid body rotation. Thus on length scales larger than the intervortex distance, the vorticity of the superfluid is essentially that of the normal fluid. In a similar fashion, the vorticity distribution due to the normal fluid eddies in a turbulent flow is matched, on average, by bundles of quantized vortices aligned on their cores. Therefore, the normal fluid vorticity is assumed comparable to the vorticity of the superfluid, and the effective density equal to the total fluid density  $\rho$ . This simple interpretation of vortex coupled superfluidity [5] is supported both by computer simulations [6] and by experiment [7]. In view of this interpretation, no difference between the behavior of decaying vorticity in He II and classical fluids is expected. Indeed, we observe no appreciable difference in turbulent decay curves obtained over a temperature range of  $1.4 < T < 2.15$  K, which corresponds to an order of magnitude difference in the normal density ratio  $\rho_n/\rho$ . We therefore analyze the decay in terms of classical HIT. Further theoretical [8] and experimental investigations of this intriguing phenomenon are presently underway and the results will be reported elsewhere.

We propose a theoretical model of decaying HIT that assumes the turbulent spectral energy density of the form shown in Fig. 1. It is generally accepted that for small wave numbers the total turbulent energy spectrum is of a form  $E(k) = Ak^m$ , with both theory [9] and experiment [10] suggesting  $m = 2$ . We assume  $A$  remains constant due to the persistence of large eddies. A similar approach that assumed validity of the Loitsianskii integral was first used in [11] (see also [9]). For large wave numbers we use Kolmogorov's prediction  $E(k) = C\varepsilon^{2/3}k^{-5/3}$ , where  $C$  is the (dimensionless) Kolmogorov constant of order unity and  $\varepsilon = -dE/dt$ . Recent investigations by Maurer and Tabeling report a Kolmogorov spectrum in both turbulent helium I and helium II [7]. These two wave number regions meet at  $k_e(t) = 2\pi/l_e(t)$ , and this peak in the energy spectrum corresponds to the energy containing eddy length scale  $l_e(t)$ , around which most of the turbulent energy resides. At large  $k$ , the spectrum is truncated at the Kolmogorov wave number  $k_\eta$  due to viscous dissipation.

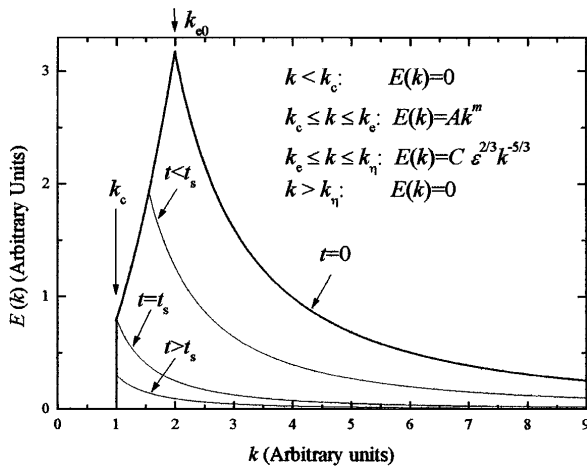


FIG. 1. Energy spectrum used in model of decaying HIT in a finite channel.

A novel aspect of our model is that we include the truncation of the spectrum at wave number  $k_c = 2\pi/d$ , attributable to the size of the containing vessel.

As the turbulence decays, the energy containing length scale grows [9], until it saturates at the size of the container at time  $t = t_s$  as shown in Fig. 1. For  $t \leq t_s$  continuity at  $k_c(t)$  gives

$$\varepsilon(t) = (A/C)^{3/2} k_e^{11/2}(t). \quad (1)$$

We evaluate the total turbulent energy as

$$E(t) = \int_{k_c}^{k_e(t)} Ak^2 dk + \int_{k_e(t)}^{k_{\eta}} C \varepsilon^{2/3} k^{-5/3} dk. \quad (2)$$

It is possible to show that due to the extremely low kinematic viscosity of helium II, simplifying the analysis by taking  $k_{\eta} \rightarrow \infty$  has little effect on the time dependence of the decay for  $\text{Re}_{\lambda} \gg 1$ . A model incorporating an arbitrary power law at low wave numbers [4], the role of viscous effects on the decay, intermittency, and a modified form of the Kolmogorov similarity law [12] will be published elsewhere.

Evaluating the integral (2) and using  $\varepsilon$  from Eq. (1) leads to

$$l_e(t) = 2\pi \left\{ \frac{5}{11} \sqrt{\frac{A}{C^3}} (t + t_0) \right\}^{2/5}, \quad (3)$$

$$\text{where } t_0 = \frac{11}{5(2\pi)^{5/2}} \sqrt{\frac{C^3}{A}} l_{e0}^{5/2}.$$

Equations (2) and (3) give the energy decay while  $l_e(t)$  grows, i.e., for  $t \leq t_s$ , where  $t_s \equiv \frac{11}{5}(2\pi)^{-5/2} \times C^{3/2} A^{-1/2} (d^{5/2} - l_{e0}^{5/2})$ , as

$$E_{<}(t) = A \left\{ \frac{11}{6} \left[ \frac{5}{11} \frac{A^{1/2}}{C^{3/2}} (t + t_0) \right]^{-6/5} - \frac{(2\pi)^3}{3d^3} \right\} \\ \approx E_0 \left( 1 + \frac{t}{t_0} \right)^{-6/5}, \quad (4)$$

where  $E_0 = (11/6)(2\pi)^3 A/l_{e0}^3$ . Application of this result to the decay of vorticity in HIT is possible via the

relationship  $\varepsilon = -dE/dt = \nu' \omega^2$  [1,13], where  $\nu'$  (a property of superfluid turbulence) is not yet known precisely, but is expected to be of the order of the kinematic viscosity of the coupled fluids, so that  $\nu' \approx \nu = \mu/\rho$ . The resulting vorticity is

$$\omega_{<}(t) = \frac{1}{\sqrt{\nu}} \left( \frac{11}{5} \right)^{11/10} C^{9/10} A^{1/5} (t + t_0)^{-11/10} \\ = \omega_{0<} \left( 1 + \frac{t}{t_0} \right)^{-11/10}, \quad (5)$$

where  $\omega_{0<} = \nu^{-1/2} (2\pi)^{11/4} (A/C)^{3/4} l_{e0}^{-11/4}$ .

For  $t \geq t_s$ , the energy containing the length scale is fixed at the size of the channel and further energy decay satisfies the familiar condition

$$\varepsilon = \frac{-dE}{dt} = 2\pi \left( \frac{2}{3C} \right)^{3/2} \frac{E^{3/2}}{l_e} = \varepsilon_0 \frac{E^{3/2}}{l_e}, \quad (6)$$

where we use  $E$  instead of the turbulent velocity variance and  $l_e$  instead of the integral length scale. Integration leads to

$$E_{>}(t) = \frac{27C^3 d^2}{2(2\pi)^2} (t + t_0 + t_1)^{-2} \quad (7)$$

and

$$\omega_{>}(t) = \frac{d}{2\pi\sqrt{\nu}} (3C)^{3/2} (t + t_0 + t_1)^{-3/2} \\ = \omega_{0>} \left( 1 + \frac{t}{t_0 + t_1} \right)^{-3/2}, \quad (8)$$

where  $t_1 = (4/5)(2\pi)^{-5/2} C^{3/2} A^{-1/2} d^{5/2}$  and  $\omega_{0>} = \frac{d}{2\pi\sqrt{\nu}} (3C)^{3/2} (t_0 + t_1)^{-3/2}$ . At  $t = t_s$ ,  $E_{<}(t_s) = E_{>}(t_s) = (2\pi)^3 3A/2d^3$ , and  $\omega_{<}(t_s) = \omega_{>}(t_s) = (2\pi)^{11/4} \nu^{-1/2} \times A^{3/4} C^{-3/4} d^{-11/4}$ .

Numerical simulations of turbulence in a periodic box using hyperviscosity in the Navier-Stokes equation also show that the integral length scale initially grows, reaches the size of the box, and remains constant thereafter [14]. The energy then decays as  $E \propto t^{-2}$ , in agreement with our model.

Typical experimental data taken at  $T = 1.5$  K, for grid velocities of 5, 10, 50, 100, and 200 cm/s, are shown as solid lines in Fig. 2. The plotted vorticity represents the superfluid vorticity averaged across the detecting volume of about  $1 \text{ cm}^3$ . At time  $t = 0$  the grid passes a predetermined reference position located 7 mm above the middle of the detecting volume. The arbitrary reference position introduces a grid velocity dependent virtual origin that slightly affects the decay slope for times  $t \ll t_s$ . The individual decay curves possess a pronounced feature (see arrows in Fig. 2) which we believe corresponds to the saturation of the energy containing the length scale at the size of the channel. We define the saturation time,  $t_s$ , as the time at which

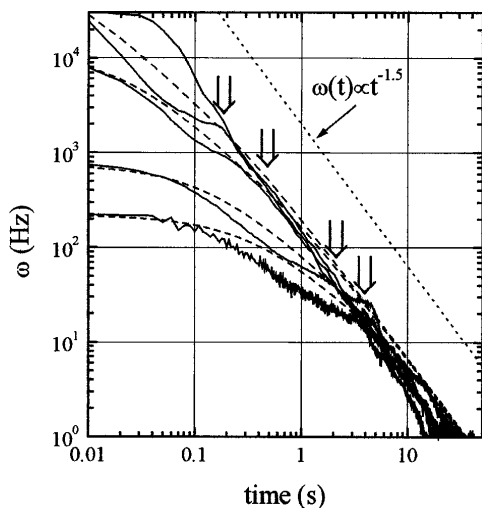


FIG. 2. Decay of vorticity for grid velocities of 5, 10, 50, 100, and 200 cm/s (top curve) at 1.5 K. Dashed lines represent model calculation.

the vorticity begins to decay as  $\omega(t) \propto t^{-3/2}$ . We also define the saturation vorticity as  $\omega_s = \omega(t_s)$ . For  $t > t_s$ , we do not observe any appreciable departure from the asymptotic decay  $\omega(t) \propto t^{-3/2}$  down to the level of a few Hz. Equation (8) leads to an experimental value of the three dimensional Kolmogorov constant  $C = 1.3 \pm 0.2$ . The fact that the experimental decay curves coincide at sufficiently long times demonstrates the independence of  $C$  (and  $\varepsilon_0$ ) from  $\text{Re}_\lambda$ .

From each set of experimental data we obtain  $t_s$ ,  $\omega_s$ , and  $\omega_{0<}$ . Experimentally we have found the relationship  $V_g t_s = X_s = 19 \pm 2$  cm. The initial vorticity can be reliably read from the decay data taken for relatively low towing velocities, where the initial decay is almost flat. Using these values we calculate  $C_m$ ,  $A$ , and  $l_{e0}$  using the following equations derived from our model:

$$C_m = \frac{5}{11} (2\pi)^{2/3} \nu^{1/3} (\omega_s)^{2/3} t_s d^{-2/3} \frac{1}{1 - (\omega_s/\omega_0)^{10/11}}, \quad (9)$$

$$A = \frac{5}{11} (2\pi)^{-3} \nu (\omega_s)^2 t_s d^3 \frac{1}{1 - (\omega_s/\omega_0)^{10/11}}, \quad (10)$$

$$l_{e0} = d (\omega_s/\omega_0)^{4/11}, \quad \text{and } t_0 = t_s \frac{(\omega_s/\omega_0)^{10/11}}{1 - (\omega_s/\omega_0)^{10/11}}. \quad (11)$$

Values of these parameters for each grid velocity are given in Table I. The dashed lines in Fig. 2 represent the associated theoretical decay curves calculated from Eqs. (5) and (8). Table I shows that the initial energy containing length scale,  $l_{e0}$ , is typically only a few times smaller than the size of the channel. That the kink in the vorticity decay indeed marks the saturation of the energy containing the length scale is supported by the value of the Kolmogorov constant,  $C_m$ , obtained from Eq. (9), is comparable with the value of  $C$  obtained from Eq. (8).

The microscale Reynolds number is calculated as  $\text{Re}_\lambda = \sqrt{15} l_e^{2/3} \nu^{-1/3} \omega^{1/3}$  [3,4]. A vorticity of 1 Hz corresponds to  $\text{Re}_\lambda \approx 85$  and  $\text{Re}_\lambda$  at the saturation time is given in Table I. No appreciable variation in  $C$  over a wide range of  $\text{Re}_\lambda$  confirms that the energy dissipation rate scales as in Eq. (6). This result is consistent with previous observations obtained for  $\text{Re}_\lambda < 550$  [13], and extends the  $\text{Re}_\lambda$  range to over  $10^3$ .

The above model is based on HIT and should therefore be considered as an approximation that, nevertheless, describes the decay curves qualitatively well. However, it does not explain the kink that is clearly present in the data just before saturation occurs, and, of course, the customary logarithmic plots tend to minimize apparent deviations in experiments covering many decades of the variables.

We have applied this model to other data on decaying grid turbulence. De Silva and Fernando studied the temporal decay of turbulence created in a water tank by a steadily oscillating grid [2]. Grid motion was suddenly stopped and the energy decay was measured using laser Doppler velocimetry some distance below the grid. Since the turbulence was fully developed, it seems justified to assume its spectral distribution has the form shown in Fig. 1. The authors give the decay data in relative units (Figs. 3 and 4 in [2]). Although absolute values of energy and time were not published, we plot the decays in the correct relative position to each other in Fig. 3. The observed energy decay is well described by Eqs. (4) and (7), and displays a changeover of power law from  $-1.2$  to  $-2$ , suggesting saturation of the energy containing length scale. We observe that this changeover takes place at a value of  $\text{Re}_\lambda \approx 50$  [2], so that the author's explanation of a final period of decay seems unlikely. Moreover, within experimental uncertainty, the data for  $t > t_s$  tend to collapse onto a universal curve as predicted by our model.

TABLE I. Parameters of the model for different grid velocities.

$\nu_g$ (cm/s)	$\omega_{0<}$ (Hz)	$\omega_s$ (Hz)	$t_s$ (s)	$t_0$ (s)	$t_1$ (s)	$A$ (cm <sup>5</sup> /s <sup>2</sup> )	$C_m$	$l_{e0}$ (cm)	$\text{Re}_\lambda(t_s)$
5	220	$18 \pm 3$	$3.5 \pm 0.2$	0.401	1.42	0.0002	1.89	0.402	216
10	750	$40 \pm 5$	$2.0 \pm 0.1$	0.150	0.782	0.0006	1.78	0.344	394
50	$1.2 \times 10^4$	$450 \pm 50$	$0.42 \pm 0.03$	0.022	0.161	0.016	1.83	0.303	658
100	$10^5$	$1850 \pm 60$	$0.17 \pm 0.02$	0.0046	0.064	0.104	1.86	0.234	1054

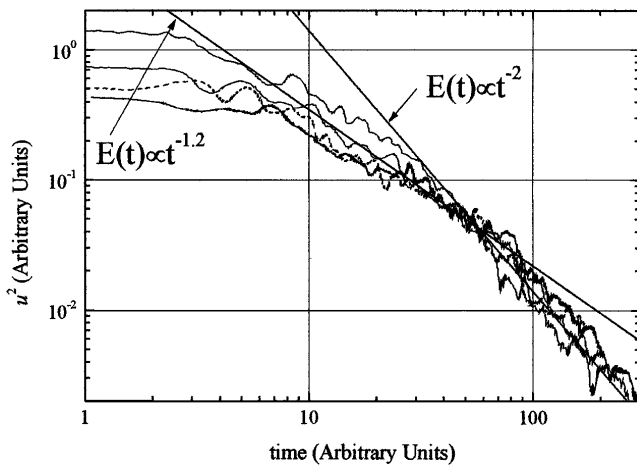


FIG. 3. Temporal energy decay of turbulence created by an oscillating grid in water [2]. Original data (Figs. 3 and 4 of [2]) have been shifted. Solid lines represent the horizontal component of the turbulent velocity measured at the depths 10.8; 14.4 and 18.7 cm below the grid position, the dashed line is the vertical component of velocity at the level 14.4 cm.

It is easy to show that saturation of the energy containing eddies in wind tunnel experiments is unlikely. As an example, consider the wind tunnel of [10] possessing a test section of  $1 \times 1.3 \text{ m}^2$ . From the experimental energy spectrum, we estimate  $A \approx 3 \times 10^3 \text{ cm}^5 \text{ s}^{-2}$ . Our simple model then predicts  $t_s \approx (11/5)(d/2\pi)^{5/2} C^{3/2} A^{-1/2} \approx 90 \text{ s}$ . With a wind speed of 10 m/s the test section would need to be nearly a kilometer long to observe saturation.

In conclusion, the ability to directly observe the superfluid vorticity over a large dynamical range gives important information about the decay of classical turbulence. Based on our data, we have developed a model of decaying classical HIT assuming a truncated energy spectrum. We predict two decay regimes possessing different energy decay rates: the first takes place when the energy contain-

ing length scale is growing, the second after it is saturated due to the size of the container. Saturation of the energy containing length scale is evident in the He II towed grid experiment as well as in classical experiments on decaying grid turbulence.

The authors acknowledge stimulating discussions with G.L. Eyink, K.R. Sreenivasan, C.J. Swanson, and W.F. Vinen, at various stages of this work. This research was supported by NSF under Grant No. DMR-9529609.

- 
- [1] See, for example, G.K. Batchelor, *The Theory of Homogeneous Turbulence* (Cambridge University Press, Cambridge, 1953); J.O. Hinze, *Turbulence* (McGraw-Hill, New York, 1975), 2nd ed.
  - [2] I.P.D. De Silva and H.J.S. Fernando, *Phys. Fluids* **6**, 2455 (1994).
  - [3] M.R. Smith, R.J. Donnelly, N. Goldenfeld, and W.F. Vinen, *Phys. Rev. Lett.* **71**, 2583 (1993).
  - [4] S.R. Stalp, Ph.D. dissertation, University of Oregon, 1998.
  - [5] R.J. Donnelly, in *High Reynolds Number Flows Using Liquid and Gaseous Helium*, edited by R.J. Donnelly (Springer-Verlag, Berlin, 1991).
  - [6] C.F. Barenghi, D.C. Samuels, G.H. Bauer, and R.J. Donnelly, *Phys. Fluids* **9**, 2361 (1997).
  - [7] J. Maurer and P. Tabeling, "Local Investigation of Superfluid Turbulence" (to be published).
  - [8] W.F. Vinen (private communication).
  - [9] P.G. Saffman, *J. Fluid Mech.* **27**, 581 (1967); *Phys. Fluids* **10**, 1349 (1967).
  - [10] G. Comte-Bellot and S. Corrsin, *J. Fluid Mech.* **48**, 273 (1971).
  - [11] G. Comte-Bellot and S. Corrsin, *J. Fluid Mech.* **25**, 657 (1966).
  - [12] L. Mydlarski and Z. Warhaft, *J. Fluid Mech.* **320**, 331 (1996).
  - [13] K.R. Sreenivasan, *Phys. Fluids* **27**, 1048 (1984).
  - [14] V. Borue and S.A. Orszag, *Phys. Rev. E* **51**, R856 (1995).